Single-optical-element soft-x-ray interferometry with a laser-plasma x-ray source

Ulrich Vogt,* Magnus Lindblom, Per A. C. Jansson, Tomi T. Tuohimaa, Anders Holmberg, and Hans M. Hertz

Biomedical and X-Ray Physics, Royal Institute of Technology/Albanova, SE-106 91 Stockholm, Sweden

Marek Wieland and Thomas Wilhein

University of Applied Sciences Koblenz, Rhein Ahr Campus Remagen, Suedallee 2, D-53424 Remagen, Germany

Received March 8, 2005

We report on a compact interferometer for the water-window soft-x-ray range that is suitable for operation with laser-plasma sources. The interferometer consists of a single diffractive optical element that focuses impinging x rays to two focal spots. The light from these two secondary sources forms the interference pattern. The interferometer was operated with a liquid-nitrogen jet laser-plasma source at $\lambda = 2.88$ nm. Scalar wave-field propagation was used to simulate the interference pattern, showing good correspondence between theoretical and experimental results. The diffractive optical element can simultaneously be used as an imaging optic, and we demonstrate soft-x-ray microscopy with interferometric contrast enhancement of a phase object. © 2005 Optical Society of America

OCIS codes: 050.1970, 340.7450, 340.7460.

X-ray interferometry is an increasingly important tool, e.g., for metrology and microscopy. Several x-ray interferometers have been developed in the recent past. Different types of interferometer have different demands on the coherence properties of the x-ray radiation, and accordingly the choice of the x-ray source is an important decision. One possibility is radiation from synchrotron sources, after applying spectral and spatial filtering.[1] However, several interferometry applications benefit from laboratory-scale instrumentation. Here compact or semicompact sources such as x-ray lasers[2] and high-harmonic sources[3] that deliver radiation with an intrinsically high degree of coherence have been employed. The use of compact laser-plasma x-ray sources has also been demonstrated.[4] However, until now interferometers at laboratory sources were limited to the extreme-ultraviolet wavelength region (down to $\lambda = 13$ nm). In this Letter we describe an interferometer for water-window soft-x-ray radiation ($\lambda = 2.88$ nm) that is based on a laser-produced plasma as the compact laboratory x-ray source. The interferometer utilizes a single focusing diffractive optical element (DOE), which also can be used as the objective in an x-ray microscope.

As the starting point for the design of our interferometer we used the concept of a zone-plate interferometer. Different arrangements of this interferometer have been demonstrated that use synchrotron radiation at $\lambda = 0.3$ nm (Ref. 5) and high-harmonic radiation near $\lambda = 13$ nm.[3] Two zone plates act as diffractive amplitude beam splitters that focus the incident radiation into two spots. These two spots form secondary sources of two spherical waves, which can interfere with each other. As an advancement of this interferometer concept we developed a single x-ray DOE that acts as a normal zone plate but produces two slightly shifted foci. Similar DOEs were introduced by DiFabrizio *et al.* for hard-x-ray ($\lambda = 0.3$ nm) synchrotron applications.[6]

For the calculation of the pattern of the interferometer's DOE we used a method similar to the one described in Ref. 6. A one-dimensional phase function Φ (modulus 2π) is calculated by wave-field propagation of two spherical monochromatic waves originating from two slightly displaced point sources. To obtain a pattern that can be produced by means of nanofabrication, we achieve a binary pattern with the conditions $0 \leqslant \Phi < \pi \Rightarrow 0$ and $\pi \leqslant \Phi < 2\pi \Rightarrow 1$; 0 indicates the area of the DOE with no material, and 1 indicates the area with material. As a final step the one-dimensional pattern is extrapolated into two dimensions with the help of symmetry considerations. The pattern appears as a normal zone plate pattern but with an overlaid linear phase grating[7] (Fig. 1, inset).

The resultant DOE is a single-element interferometer and is therefore extremely compact and insensitive to vibrations. Another major advantage is the moderate coherence requirements. It follows from geometrical considerations that only an area with the diameter of the spot separation distance must be illuminated spatially coherently. For the temporal co-

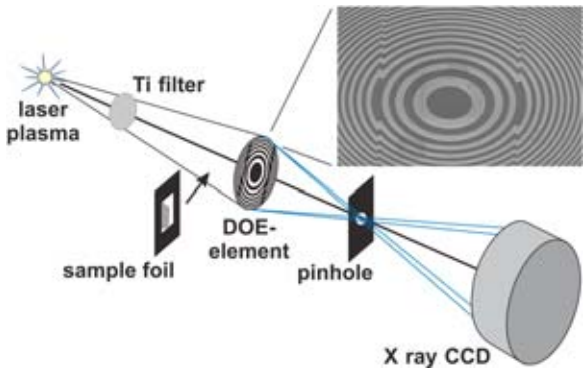

Fig. 1. Arrangement of the interferometer experiment. Inset, electron microscope image of the inner part of the DOE. Note the reversal of the zones in the left and right parts of the image.

0146-9592/05/162167-3/$15.00

herence or coherence length, which is dependent only on monochromaticity $\lambda/\Delta\lambda$ of the radiation,[1] the same criterion applies as for a normal zone plate when it is used as an imaging optics. The monochromaticity should be of the order of the number of zones of the zone plate.[1]

Based on the considerations mentioned above, we calculated a DOE, using a code written in Matlab. The design parameters of the DOE are a 75 μm diameter, a 3 mm focal length for a wavelength of 2.88 nm, and a spot size separation of 600 nm. This configuration results in 160 zones and an outermost zone width of ~100 nm. The code directly generates a file for an *e*-beam lithography system that uses a polygonial path mode with a data file resolution of 1 nm. Details of the nanofabrication process can be found in Ref. 8. The resultant DOE is fabricated on a 50 nm Si_3N_4 membrane and consists of ~150 nm electroplated nickel.

Figure 1 shows the complete interferometer arrangement. The plasma was produced in a liquid-nitrogen jet with a frequency-doubled Nd:YAG laser (Coherent Infinity; pulse duration, 3 ns) at a pulse energy of ~115 mJ. Details of the characteristics of the laser plasma were published elsewhere.[9] A 300 nm thick titanium foil isolated one emission line at $\lambda = 2.88$ nm from the rest of the spectrum emitted by the plasma. Therefore the coherence length of the x rays passing through the filter was determined by the linewidth of the emission line itself, which was well above the needed monochromaticity of $\lambda/\Delta\lambda > 160$. The x-ray-emitting diameter of the plasma was ~20 μm (FWHM).[9] By placing the DOE 25.7 cm from the plasma, we calculated the diameter of the spatially coherently illuminated field to be ~12 μm,[10] well above the spot separation of 600 nm. A pinhole with a diameter of 20 μm was located in the focal plane of the DOE (+1st order) to block other diffraction orders than +1st order. A central stop was used to cut out the 0th order on the x-ray CCD detector (Andor Technologies; 13 μm $\times$ 13 μm pixel size). The distance between pinhole and CCD was 24.5 cm. To prevent absorption of the x-ray radiation we placed the source and the complete optical arrangement in vacuum at a pressure below 7.5×10^{-5} Torr.

A CCD image of the interferogram obtained is shown in Fig. 2. It exhibits a basic modulation with a period of 1.2 mm, which is the expected period given the spot separation and distance to the detector. Moreover, the interferogram also contains additional modulations with higher frequencies (Fig. 2, bottom). To explain the formation of the pattern we performed a one-dimensional simulation by scalar wave-field propagation. A plane monochromatic wave was propagated through both a DOE pattern of the perfect phase map Φ and the manufactured binary DOE pattern. The resultant intensities in the focal plane of the DOE (+1st order) and in the detector plane are plotted in Fig. 3. The perfect phase map leads to two single spots and accordingly to a sinusoidal modulation of the intensity in the interferogram. However, in the focal plane of the real binary DOE a number of side peaks appear in addition to the two main spots.

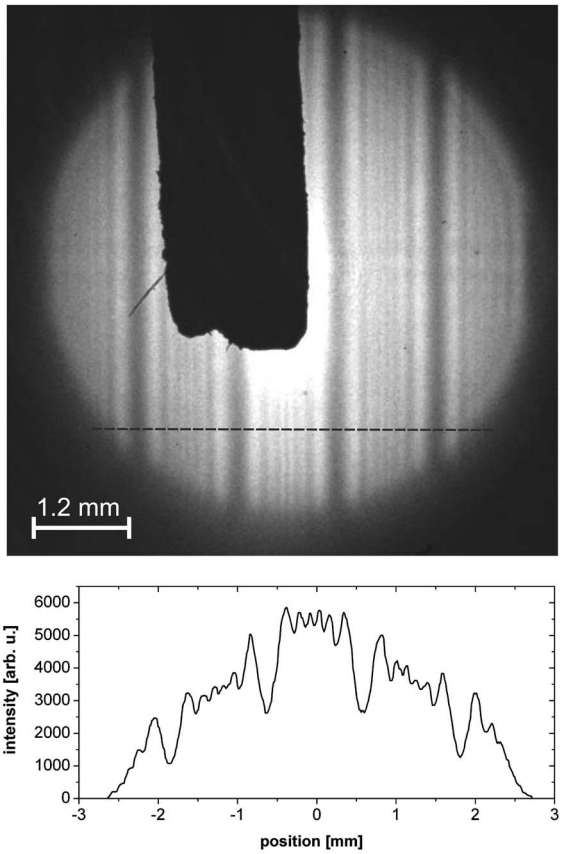

Fig. 2. Top, interferogram obtained from the CCD detector with an exposure time of 120 s. Dashed line, position of the line plot through the image that is shown below. The large black shadow is the central stop to block the 0th order.

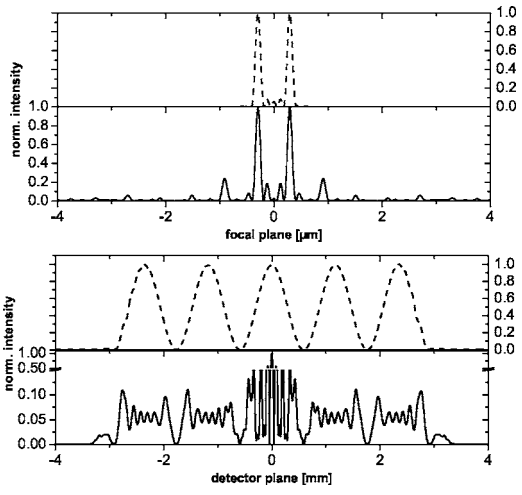

Fig. 3. One-dimensional simulation of the intensity in the focal plane of the DOE (top) and on the CCD (bottom). Dashed curves, results, for the perfect phase map; solid curves, for the binary manufactured pattern.

These are a direct consequence of the binary nature of the DOE pattern and can be regarded as higher orders of the overlaid linear phase grating. Thus these side peaks lead to modulations with higher frequencies in the interferogram as plotted in Fig. 3. A com-

parison of the simulated and measured interferograms shows good qualitative agreement. Note that the line plot in Fig. 2 (bottom) is located at a position where the central stop does not obscure the image while the simulation shows the result for the center of the interferometer, including the 0th order. The modulation contrast of the intensity in the measured interferogram is reduced because the DOE is not illuminated with a plane wave as assumed in the simulation. Moreover, the decrease of the intensity toward the outer part of the interferogram reproduces the emission profile of the plasma source.

Because the DOE not only is an amplitude beam splitting element but also works as an x-ray objective, a sample was placed in front of the DOE (Fig. 1) so that an image on the detector was formed. As a test sample a 50 nm Si_3N_4 membrane was evaporated with 400 nm chromium and cracked to yield a sharp edge. The magnification of the arrangement was 81×. A detail of an image obtained is shown in Fig. 4. The foil is visible at the left, the right-hand part of the figure contains the background, which is the unobscured interferogram, in this case a part of a large dark fringe. The resolution in the image was ~321 nm. This is slightly below the spot size separation and can explain the fact that the image of the foil in the horizontal direction, i.e., the spot separation direction, seems not to be completely sharp. Radiation from the two main focal spots form two independent images, which overlap in the detector plane. However, this effect leads to the situation that in the image of the foil edge parts of the illuminating light field passing and bypassing the sample interfere with each other. Therefore a dark and a bright fringe can be observed at the foil edge (arrow in Fig. 4), similar to that produced by differential interference contrast microscopy. In fact, successful differential interference contrast x-ray microscopy in the hard-x-ray range with a single DOE used as an objective was recently reported.[6,11]

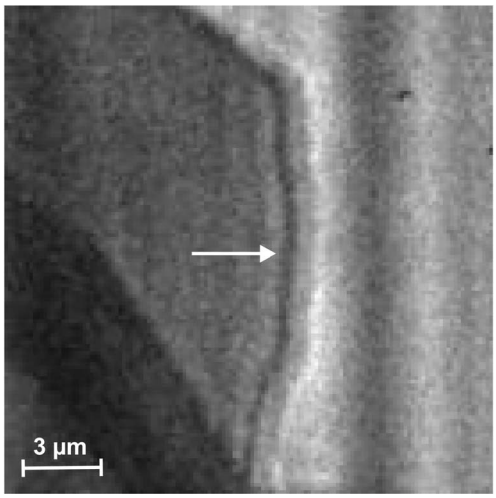

Fig. 4. Image detail of a cracked 50 nm Si_3N_4 membrane edge (arrow) covered with 400 nm of chromium. The exposure time was 60 s.

In summary, we have presented the successful design, manufacturing, and testing of a diffractive optical element as a single-element interferometer for operation at water-window soft-x-ray wavelengths. The DOE will be the basis for advanced interferometric experiments in the soft-x-ray range, especially in combination with laser-plasma sources. For this source the moderate coherence requirement of this kind of DOE is of major importance. A first promising application seems to be x-ray differential interference microscopy in the water-window spectral range with a compact laboratory x-ray microscope[12] because the DOE has the same efficiency as a normal corresponding zone plate but can provide interferometric contrast enhancement, especially for thin objects.

This project was partly funded by the Deutsche Forschungsgemeinschaft under contract WI 1451/3-1 and by the Goeran Gustafsson Foundation. U. Vogt's e-mail address is ulrich.vogt@biox.kth.se.

*Present address, University of Applied Sciences, Rhein Ahr Campus, Remagen, Germany.

References

1. D. Attwood, *Soft X-Rays and Extreme Ultraviolet Radiation* (Cambridge U. Press, 1999).
2. H. Daido, Rep. Prog. Phys. **65**, 1513 (2002).
3. M. Wieland, T. Wilhein, C. Spielmann, and U. Kleineberg, Appl. Phys. B **76**, 885 (2003).
4. A. K. Ray-Chaudhuri, K. D. Krenz, R. P. Nissen, S. J. Haney, C. H. Fields, W. C. Sweatt, and A. A. MacDowell, J. Vac. Sci. Technol. B **14**, 3964 (1996).
5. T. Wilhein, B. Kaulich, and J. Susini, Opt. Commun. **193**, 19 (2001).
6. E. DiFabrizio, D. Cojoc, S. Cabrini, B. Kaulich, J. Susini, P. Facci, and T. Wilhein, Opt. Express **11**, 2278 (2003).
7. T. Weitkamp, O. Dhez, B. Kaulich, and C. David, Proc. SPIE **5539**, 195 (2004).
8. A. Holmberg, S. Rehbein, and H. M. Hertz, Microelectron. Eng. **73–74**, 639 (2004).
9. P. A. C. Jansson, U. Vogt, and H. M. Hertz, Rev. Sci. Instrum. **76**, 043503 (2005).
10. M. Born and E. Wolf, *Principles of Optics* (Cambridge U. Press, 1980).
11. T. Wilhein, B. Kaulich, E. DiFabrizio, F. Romanato, S. Cabrini, and J. Susini, Appl. Phys. Lett. **73**, 2082 (2001).
12. M. Berglund, L. Rymell, M. Peuker, T. Wilhein, and H. M. Hertz, J. Microsc. **197**, 268 (2000).